

Energy Prediction During Approach and Landing Based on Long Short-Term Memory Model

Jiaqi Yan^{1,*}

¹School of Aeronautics, Northwestern Polytechnical University, Xi'an 710072, China ^{*}Contact author: Jiaqi Yan. E-mail: 1608354921@qq.com.

Abstract

Statistical analysis of civil aircraft accidents shows that the highest accident rate occurs during the approach and landing phase. The main feature of these accidents is abnormal energy state, which leads to critical situations such as stall and hard landing. Therefore, accurately predicting the energy state of an aircraft during the approach and landing phase is of great significance to ensure the safe landing of the aircraft. This paper proposes a deep learning method for predicting the energy state of an aircraft during approach and landing based on time series data. First, through an extensive review of existing literature, three characteristic parameters, namely altitude, speed, and glide angle, are selected as indicators to characterize the energy state. On this basis, a semi-physical simulation platform for a certain type of aircraft is developed. Approach and landing experiments with different throttle sizes and flap deflections are carried out under different wind speeds and wind directions. Then, based on the experimental data, a deep learning prediction model based on long short-term memory (LSTM) is established to predict the energy state indicators during the approach and landing phase. Finally, the established LSTM model is rigorously trained and tested under different strategies, and a comparative analysis is performed. The results show that the proposed LSTM model has high accuracy and strong generalization ability for predicting the energy state of the aircraft during the approach and landing phase. The research results provide a theoretical basis for designing energy warning systems and formulating flight control laws during approach and landing phases.

Keywords: Approach and landing; Energy state; LSTM; State prediction; Flight safety

1. Introduction

Recent accident data on civil aviation highlights that the approach and landing phase with gradually decreasing energy is the phase most prone to accidents, as shown in Figure 1 [1-3]. One of the key causes of forced landing accidents is improper aircraft energy management; abnormal energy approach and landing is the main cause of further accidents such as stalls, hard landings, and runway departure accidents [4-6]. Most modern fly-by-wire aircraft exhibit neutral speed stability, making it challenging for pilots to directly discern speed changes using the joystick. This difficulty often leads to a transition to an abnormal energy state, as described in [7]. The key parameters for identifying abnormal energy conditions during the approach and landing phases have been identified as velocity, glide angle, altitude, and descent rate.

Given the complexity and barriers of analog approaches to accurately locate and predict abnormal energy states, data mining and deep learning techniques have emerged as promising alternatives. In the field of data mining, anomaly detection involves identifying patterns in data that deviate from predefined norms or expectations [8,9]. Aviation safety analysts are particularly interested in two different types of flight anomalies: transient anomalies and flight-level anomalies. Transient anomalies are characterized by a short period of abnormal events in a flight record [10,11], while flight-level anomalies are characterized by persistent abnormal data patterns that span an entire flight or a specified flight phase [12,13].

This study proposes an LSTM-based method to predict the energy state of aircraft during the approach and landing stages. This method involves analyzing the changes in flight parameters that

Energy Prediction During Approach and Landing Based on LSTM Model

represent the energy state of the aircraft and building a prediction model based on LSTM theory. To build this model, this study first identified the relevant flight parameters through a comprehensive literature review. These parameters were then collected by semi-physical simulation tests using an aircraft flight simulator under the guidance of the flight manual. The simulator replicated real flight conditions at different throttle settings, wind speeds, and wind directions. Finally, the LSTM model was built and trained using the collected flight parameters to predict the energy state during the approach and landing phases. The model facilitates the perception, control, and correction of abnormal energy states, thereby improving flight safety.

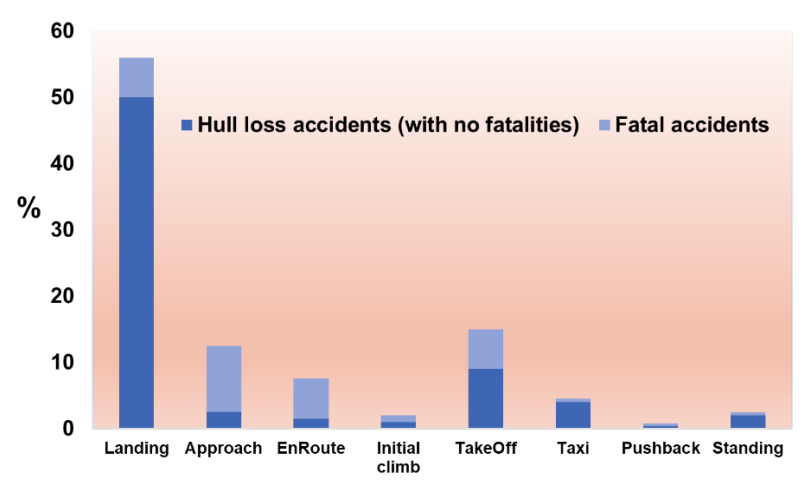


Figure 1 - Accident distribution per flight phase 2002-2022.

2. Basis of Aircraft System Reliability Modeling

At present, there are many research results on the indicators that characterize the energy state of the aircraft during the approach and landing phases, as shown in Table 1. Based on these research results, three key flight parameters, including speed, altitude, and glide angle, were selected to characterize the energy state of the aircraft. In this study, speed refers to the aircraft's indicated airspeed, and altitude refers to the radio altitude.

Table 1 - Summary of research results representing aircraft energy state.					
Energy state indicators in the approach and landing phase	Sources of literature				
Velocity deviation, glide path deviation, descent rate	Flight Safety Foundation (FSF)				
Velocity criterion for identifying low kinetic energy, slip deviation criterion for identifying low potential energy	From the airworthiness regulatory requirements				
Velocity and altitude	Aircraft mode and energy-state prediction, assessment, and alerting				
Velocity deviation, glide path deviation	Robust autopilot design for landing a large civil aircraft in crosswind				
Nominal profile deviation and data analysis, and data comes from the high-fidelity simulation model and aircraft operation data	CCAR Approach and landing procedure of large transport civil aircraft				
Kinetic energy, potential energy, total energy, and their rate of change	Energy-based metrics for safety analysis of general aviation operations				

The warning boundary of abnormal energy can be summarized as follows:

$$\begin{cases} -5 \text{ kts} < V - V_{\text{ref}} < 20 \text{ kts} \\ -1 \text{ dot} < \gamma - \gamma_0 < 1 \text{ dot} \\ V \text{sin} \gamma > -1,000 \text{ ft/min} \end{cases}$$

In the criteria above, 1 dot \approx 0.35°; γ_0 = 3°; V is the velocity that indicates the indicated airspeed; V_{ref} refers to the Reference Landing Speed, with its general value being 1.3 V_{so} and with V_{so} being the

stall speed in the aircraft landing configuration. Energy states exceeding the range above are considered to be abnormal energy states in the approach and landing phases.

3. Simulation and Prediction Models of Approach and Landing

3.1 Simulation Experiment Based on Flight Simulator

In this study, the experimental platform uses human-computer interaction to simulate flight approach and landing. The experimental plan is as follows: (1) According to the flight manual, set up multiple groups of flight experiments based on throttle size, flap deflection, wind speed, wind direction, turbulence, etc.; (2) Initialize the approach and landing state of the aircraft, and then simulate the approach and landing phases of the aircraft through human-computer interaction methods such as pulling/pressing the joystick and sliding the platform throttle; (3) Record the aircraft flight parameters in the simulator at all times. The human-computer interaction platform is shown in Figure 2.



Figure 2 - Parameter panel and operating console of the semi-physical simulation platform.

In order to obtain approach and landing samples in a real flight environment, the simulation experiment is divided into three groups: no wind, wind and turbulence. According to Table 2, the wind speed can be set as 2m/s, 4 m/s, 6 m/s, 8 m/s, 10 m/s respectively, and the wind direction is set as downwind (0°), upwind (180°), and crosswind (90°). The throttle is set as 50%, 60%, 70%, and 80%. Flaps are set as 10° and 35°. In this type of flight simulator, each 0.01s of simulation time is a sampling point. The data collected in this experiment is used for subsequent training and testing of the LSTM prediction model.

Table 2 - Speed limit values of different wind directions.

Table 2 - Opeca little values of afficient with a freedome.					
Wind direction	Wind speed				
Crosswind	25 knots (13m/s, 46km/h, indicated airspeed)				
Upwind	40 knots (20m/s, 74km/h, indicated airspeed)				
Downwind	20 knots (10m/s, 37km/h, indicated airspeed)				

3.2 Prediction Model Based on LSTM

Figure 3 shows the architecture of the LSTM model used in this study to predict the speed, altitude, and glide angle during the approach and landing phases of an aircraft. Each colored circle represents a node in the LSTM layer. The number of layers and nodes in each layer are carefully adjusted through rigorous training experiments. These models take the values of flight parameters at a specific time interval, denoted as x(t), to predict the corresponding altitude, speed, or glide angle at a future time, denoted as y(t). In the LSTM context, x(t) and y(t) are called feature quantities and label quantities, respectively. The step time Δr of the model can be flexibly set, and the prediction time step k can also be varied as needed. This approach can make accurate predictions based on a wide range of flight parameters and time intervals. In this paper, the final trained model architecture

consists of an LSTM layer with 20 nodes.

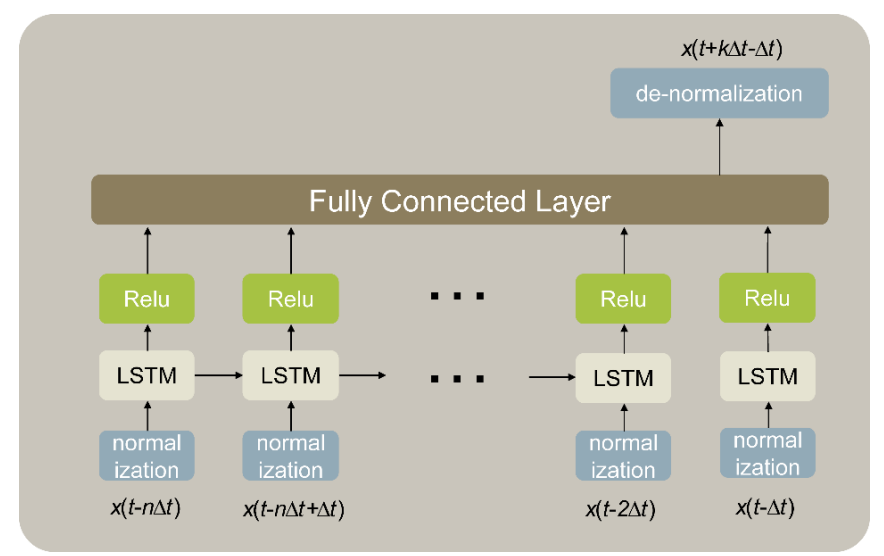


Figure 3 - LSTM model for energy state prediction of approach and landing.

As shown in Figure 4, before training and testing the designed LSTM model, the samples need to be preprocessed and normalized. Preprocessing includes conventional processing such as data cleaning, padding, and smoothing. In addition, in order to solve the dimensional differences in the data, accelerate model convergence, improve prediction accuracy, and enhance the generalization ability of the model, this study normalized the feature quantity (as the input of the model) and the label quantity (representing the output of the model) before introducing them into the LSTM architecture. All datasets were specially scaled to limit their values to [0,1]. In addition, this paper uses the Adam gradient descent method to train LSTM. Adam can adaptively adjust the learning rate, prevent overfitting to a certain extent, and make the convergence effect better.

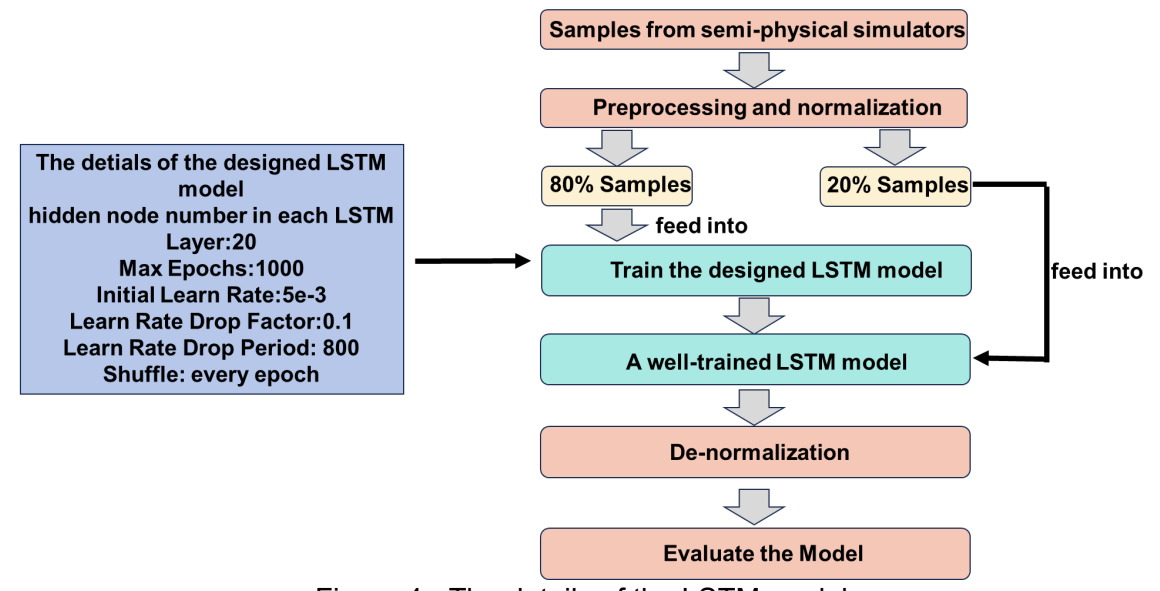


Figure 4 - The details of the LSTM model.

4. Experiments of LSTM on the Flight Data

4.1 Strategies for Training and Testing LSTM

A total of 80 approach and landing experiments were conducted in this study, including three working conditions: no wind, wind, and turbulence. The time series data of flight parameters in each flight experiment were recorded in a file. The sampling frequency of each flight was 100 Hz, and 80 record files were formed in the flight simulator. The process from the initial approach state to the aircraft touching the ground was about 150 seconds, that is, through an approach and landing flight experiment, there were about 15,000 rows of data in each record file. The most basic condition for the approach and landing stage is no wind. Therefore, taking the no wind condition as a typical case,

according to the principle that the generalization ability of the prediction model is from medium to strong, six strategies for training and testing the designed LSTM are proposed.

- (1) Randomly select a single wind-free file without perturbing the time sequence of data in the file; divide the data in the file into 8:2 as a training set and test set, respectively.
- (2) Randomly select a single wind-free file; randomly mix up the time sequence of data in the file; divide the data in the file into 8:2 as a training set and test set, respectively.
- (3) Randomly select a single wind-free file; sparse the data in the file as follows: 1 in every 10 raw data is kept as a sample; randomly disorder the time sequence of these samples; divide the samples into 8:2 as a training set and test set, respectively.
- (4) Select all the wind-free files; sparse the data in each file as follows: 1 in every 100 raw data is kept as a sample; randomly shuffle the time sequence of all the samples in the files; divide the samples into 8:2 as a training set and test set, respectively.
- (5) Randomly select eight files including the wind and wind-free conditions for training and select one wind file and one wind-free file for testing; sparse the data in each file as follows: 1 in every 100 raw data is kept as a sample; randomly disarrange the time sequence of the samples in the training set, and do not disarrange the time sequence of samples in the test set.
- (6) Randomly select 56 files including the wind, wind-free, and turbulent conditions for training, and select 14 files including the wind, wind-free, and turbulent conditions for testing; sparse the data in each file as follows: one in every 100 raw data is kept as a sample; randomly disorder the time sequence of the samples in the training set, and do not disorder the time sequence of samples in the test set.

4.2 Result Analysis

This study evaluates the performance of LSTM based on the indicators of R-square (R²), Mean Absolute Error (MAE), and Mean Bias Error (MBE). R² is the coefficient of determination, and its value range is 0 to 1. The closer it is to 1, the more accurate the model is. MAE indicates the error level of the model; the lower the MAE, the more accurate the LTMS. MBE indicates the deviation direction of the model. A positive MBE indicates that the LSTM model overestimates the true value; a negative value indicates that the model underestimates the true value; and a value close to 0 indicates that the model deviation is the average value. This paper only gives the training and testing results of LSTM for predicting velocity indicators under 6 strategies (shown in Figures 5-7 and Table 3).

Table 3 - Velocity prediction of LSTM under different strategies.

Table 5 - Velocity prediction of Eo Tivi direct different strategies.									
Strategy	Strategy Parameter	Indices of Model	LSTM Method		VAR Method				
		Quality	Training Set	Test Set	Training Set	Test Set			
1	$n = 20, k = 1, \Delta t = 0.01$	R ²	0.999960	0.038281	0.919961	0.025812			
		MAE	0.033427	18.30630	0.145758	20.67242			
		MBE	-0.011397	18.30630	-0.282941	21.28936			
2 n	$n = 20, k = 1, \Delta t =$	R^2	0.999950	0.999950	0.899952	0.889947			
		MAE	0.091720	0.092625	0.275299	0.296551			
	0.01	MBE	0.018886	0.015178	0.129375	0.121329			
3 n=		R^2	0.999400	0.999290	0.909424	0.899261			
	$n = 20, k = 1, \Delta t = 0.1$	MAE	0.288590	0.291230	0.702818	0.728703			
		MBE	-0.006848	0.003985	0.306001	0.405864			
4	$n = 20, k = 3, \Delta t = 1$	R^2	0.994890	0.994030	0.894941	0.883791			
		MAE	0.763620	0.771280	4.723623	4.326705			
		MBE	0.128520	0.109820	0.810808	0.824212			
5	$n = 20, k = 3, \Delta t = 1$	R^2	0.993760	0.992720	0.914259	0.912721			
		MAE	0.840780	0.737380	1.958741	1.984753			
		MBE	0.141060	0.134040	0.329649	0.362082			
6	$n = 20, k = 3, \Delta t = 1$	R^2	0.986040	0.989760	0.956179	0.939248			
		MAE	1.373400	1.803200	1.904735	2.611392			
		MBE	0.126260	-0.083124	0.318684	0.264489			

In these figures, the horizontal axis represents the serial number of the sample. The vertical axis

Energy Prediction During Approach and Landing Based on LSTM Model

represents the value of the flight parameter to be predicted. Since each figure contains a large amount of sample data, showing the true values and predicted results of all sample points will make the image visually confusing and difficult to read, especially for the training and test results under the time series disorder strategy. This lack of clarity will hinder the reader's ability to evaluate the consistency between the model training results and the true values of the samples. Therefore, after the model is trained and tested with samples, the sample points in the figure are sparsely processed in order to present the training and test results more clearly.

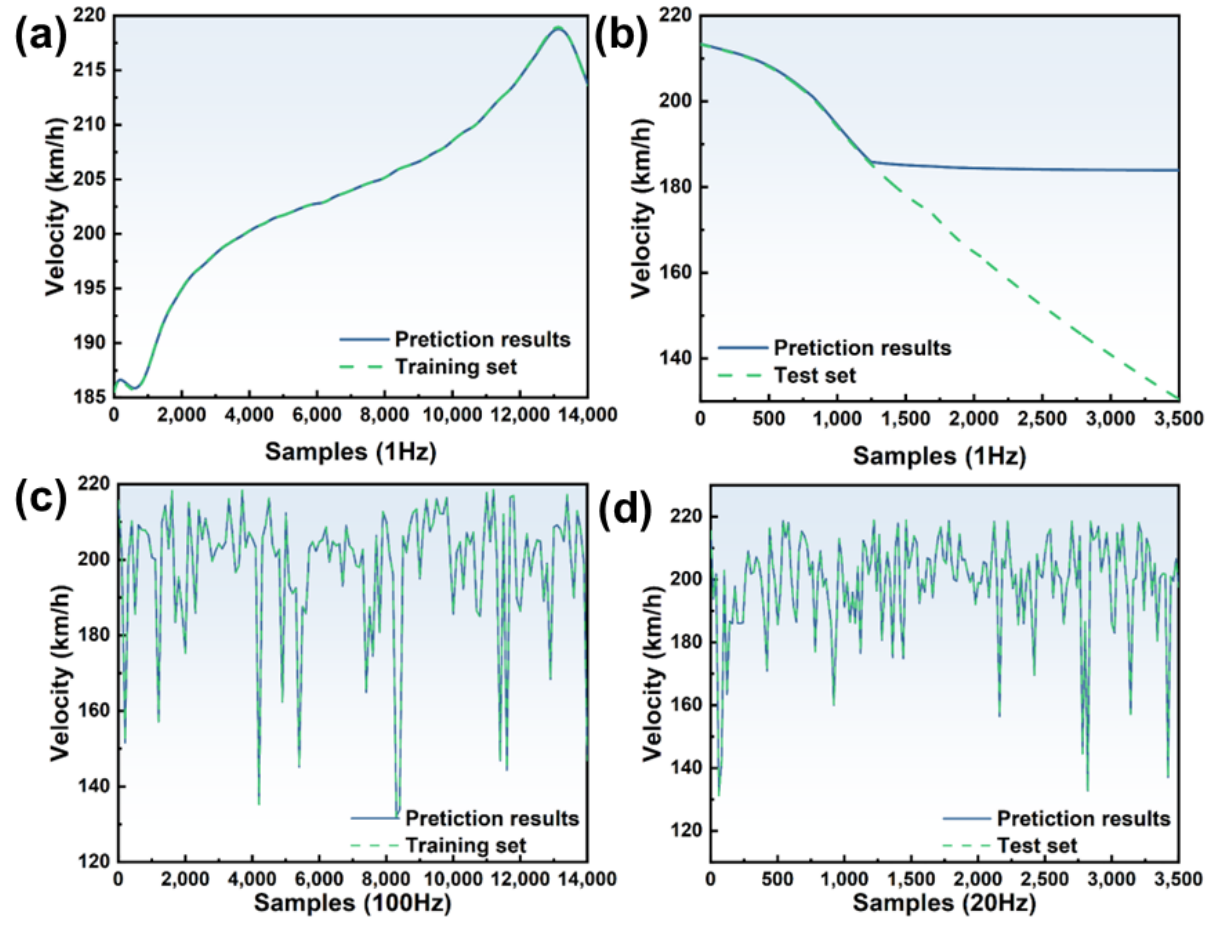


Figure 5 - Prediction results in (a) training and (b) the test set under Strategy 1. Prediction results in (c) training and (d) test set under Strategy 2.

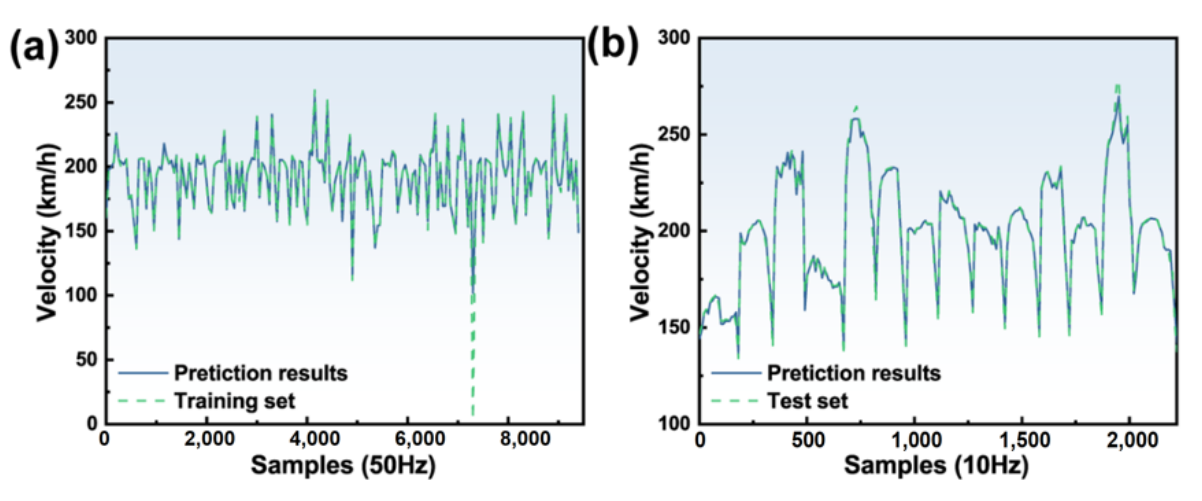


Figure 6 - Prediction results in (a) training and (b) test set under Strategy 6.

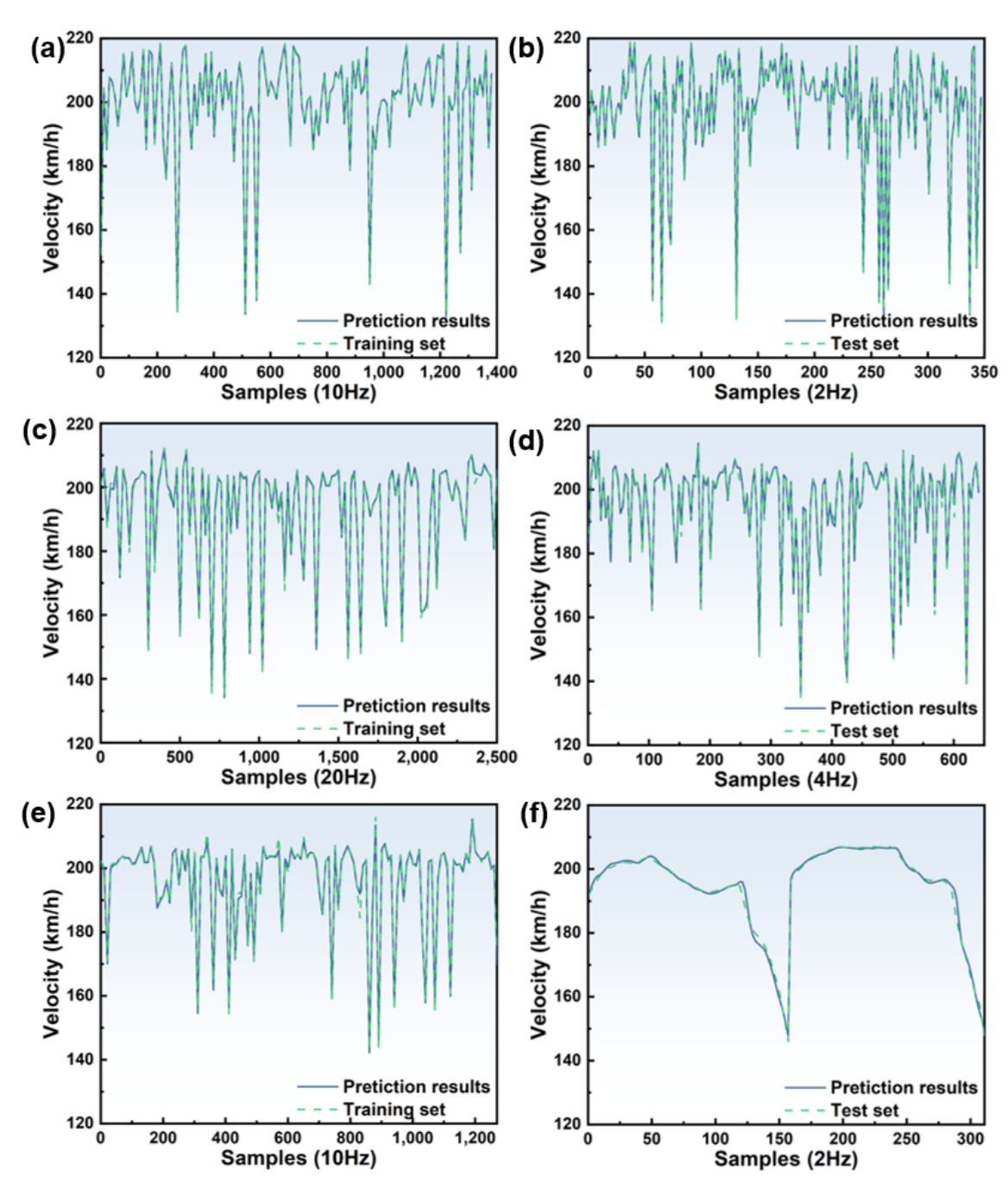


Figure 7 - Prediction results in (a) training and (b) test set under Strategy 3, those in (c) training and (d) test set under Strategy 4, and those in (e) training and (f) test set under Strategy 5.

5. Conclusions

The approach and landing phases are generally recognized as the phases with the highest incidence of civil aviation accidents. Abnormal energy states are an important cause of these accidents. Therefore, accurately predicting the energy state indicators at each stage is of great significance for guiding pilots to land safely and accurately.

- (1) A semi-physical simulation platform with integrated human-computer interaction has been developed for specific aircraft models, which overcomes the shortcomings of traditional pure digital simulation methods that are difficult to consider the impact of pilots on flight quality. The platform can also conduct approach and landing simulation experiments close to the real flight environment under three environmental conditions: calm, windy, and turbulent. Comprehensive and sufficient flight parameters can be obtained in a short time, and deep learning models with strong generalization ability can be trained.
- (2) The established LSTM-based deep learning model has a high prediction accuracy for energy

Energy Prediction During Approach and Landing Based on LSTM Model

state indicators. The R2 value of the altitude prediction model is greater than 0.99, the R2 value of the speed prediction model is greater than 0.98, and the R2 value of the glide angle prediction model is greater than 0.98. The model has strong generalization ability, and the established LSTM model can better predict the speed, altitude and glide angle of the aircraft under different wind and turbulence conditions in the next 3 seconds. This prediction strength is invaluable for early detection of abnormal energy states and for designing tailored control laws to manage and correct such states.

(3) In order to improve the prediction accuracy of LSTM, a training strategy for disordering the sample time series is proposed. The training results show that if a deep learning network for flight parameter prediction during the aircraft approach and landing phase is to be built, the time series of training samples should be disordered. Failure to do so may lead to the "overfitting phenomenon", which is characterized by high accuracy on the training set but poor performance on the test set. This finding is not only crucial for optimizing LSTM models, but also has important implications for developing other types of deep neural networks.

6. Contact Author Email Address

The contact author E-mail address: 1608354921@qq.com.

7. Copyright Statement

The authors confirm that we and our organization hold copyright on all of the original material included in this paper. The authors also confirm that we have obtained permission from the copyright holder of any third party material included in this paper to publish it as part of their paper. The authors confirm that we give permission for the publication and distribution of this paper as part of the ICAS proceedings or as individual off-prints from the proceedings.

References

- [1] Noort, M.C.; Reader, T.W.; Gillespie, A.J.S.s. Safety voice and safety listening during aviation accidents: Cockpit voice recordings reveal that speaking-up to power is not enough. *Saf. Sci.* **2021**, *139*, 105260.
- [2] Cao, E.; Dong, Z.; Zhang, X.; Zhao, Z.; Zhao, X.; Huang, H. Mechanical properties and failure analysis of 3D-printing micron-scale ceramic-based triply periodic minimal surface scaffolds under quasi-static-compression and low-speed impact loads. *Compos. Sci. Technol.* **2023**, *243*, 110248.
- [3] Kalagher, H.; de Voogt, A.; Boulter, C.J.A.P.; Factors, A.H. Situational Awareness and General Aviation Accidents. *Aviat. Psychol. Appl. Hum. Factors* **2021**, *11*, 112–117.
- [4] Perboli, G.; Gajetti, M.; Fedorov, S.; Lo Giudice, S. Natural Language Processing for the identification of Human factors in aviation accidents causes: An application to the SHEL methodology. *Expert Syst. Appl.* **2021**, *186*, 7.
- [5] Jia, B.; Huang, H.; Dong, Z.; Ren, X.; Lu, Y.; Wang, W.; Zhou, S.; Zhao, X.; Guo, B. Degradable biomedical elastomers: paving the future of tissue repair and regenerative medicine. *Chem. Soc. Rev.* **2024**, *53*, 4086–4153.
- [6] Chang, M.; Huang, L.; You, X.Q.; Wang, P.; Francis, G.; Proctor, R.W. The black hole illusion: A neglected source of aviation accidents. *Int J Ind Erg.* **2022**, *87*, 7.
- [7] Zajdel, A.; Krawczyk, M.; Szczepanski, C. Pre-Flight Test Verification of Automatic Stabilization System Using Aircraft Trimming Surfaces. *Aerospace* **2022**, *9*, 11.
- [8] Li, L.; Das, S.; John Hansman, R.; Palacios, R.; Srivastava, A.N. Analysis of flight data using clustering techniques for detecting abnormal operations. *J. Aerosp. Inf. Syst.* **2015**, *12*, 587–598.
- [9] Chandola, V.; Banerjee, A.; Kumar, V. Anomaly Detection: A Survey. ACM Comput. Surv. 2009, 41, 1–58.
- [10] Puranik, T.G.; Mavris, D.N. Identification of instantaneous anomalies in general aviation operations using energy metrics. *J. Aerosp. Inf. Syst.* **2020**, *17*, 51–65.
- [11] Li, G.; Cao, E.; Jia, B.; Zhang, X.; Wang, W.; Huang, H. Mechanical properties and failure behaviors of T1100/5405 composite T-joint under in-plane shear load coupled with initial defect and high-temperature. *Compos. Struct.* **2023**, 324, 117722.
- [12] Matthews, B.; Das, S.; Bhaduri, K.; Das, K.; Martin, R.; Oza, N. Discovering anomalous aviation safety events using scalable data mining algorithms. *J. Aerosp. Inf. Syst.* **2013**, *10*, 467–475.
- [13] Hu, Y.; Yan, J.; Cao, E.; Yu, Y.; Tian, H.; Huang, H. Approach and Landing Energy Prediction Based on a Long Short-Term Memory Model. *Aerosp.* **2024**, *11*, 226.